NACA RM L52D15a

RESEARCH MEMORANDUM

SOME EFFECTS OF FIN PLAN FORM ON THE STATIC STABILITY OF FIN-BODY COMBINATIONS AT MACH NUMBER 4.06

By Edward F. Ulmann and Robert W. Dunning

Langley Aeronautical Laboratory
Langley Field, Va.

NATIONAL ADVISORY COMMITTEE
FOR AERONAUTICS

WASHINGTON

July 2, 1952
Declassified April 8, 1957

NATIONAL ADVISORY COMMITTEE FOR AERONAUTICS

RESEARCH MEMORANDUM

SOME EFFECTS OF FIN PLAN FORM ON THE STATIC STABILITY OF FIN-BODY COMBINATIONS AT MACH NUMBER 4.06

By Edward F. Ulmann and Robert W. Dunning

SUMMARY

In order to investigate some effects of fin plan form on the static stability of fin-body configurations, tests were conducted at Mach number 4.06 on fineness-ratio-9 and -12 bodies of revolution alone and in combination with low-aspect-ratio tail fins of three plan forms having equal exposed areas. The plan forms were rectangular, delta, and the trapezoidal plan form of the vertical stabilizer of the Bell X-2 airplane. Normal-force and pitching-moment coefficients were obtained through an angle-of-attack range of 0° to 10° at Reynolds numbers of 16.8×10^6 and 22.3×10^6 based on body lengths.

It was found that the normal-force and pitching-moment coefficients of the test configurations could be predicted rather well by combining the results of a correlation of experimental data for the body alone with theoretical fin and fin-body interaction forces. The trapezoidal-finned configurations showed the most longitudinal stability, since they had the highest normal-force-curve slopes and the most rearward centers of pressure. They were followed in order of decreasing stability by the rectangular and the delta-finned configurations. It was found that the centers of pressure of the three configurations varied as the location of the centroids of fin-plan-form area.

INTRODUCTION

As the speeds of supersonic airplanes and guided missiles are increased, the wider range of operating Mach numbers for a given configuration may increase the problems of static stability. A decrease in the stability of body-tail configurations occurs as Mach number increases, since the unstable moment contribution of most bodies of revolution remains nearly constant with increasing Mach number, whereas the stabilizing moment of the fins decreases with Mach number. The rate of decrease of stability can be lessened by the use of configurations

having high-fineness-ratio noses and properly designed low-aspect-ratio control surfaces, but even with good design the stability of a configuration would probably still decrease somewhat with Mach number so that the highest flight Mach number would be the critical point.

A specific problem of this type is presented by the decrease in directional stability with Mach number of the Bell X-2 airplane as determined experimentally at Mach numbers from 1.40 to 2.32 (ref. 1). Since this decrease in directional stability is due in large part to the decreasing lift-curve slope of the vertical tail, a preliminary investigation was undertaken to determine the effects of tail-fin plan form on the static longitudinal stability of fin-body configurations at Mach number 4.06. The plan forms investigated were the trapezoidal plan form of the vertical stabilizer of the Bell X-2 airplane of aspect ratio 2.384, and rectangular and delta plan forms of aspect ratio 1.72. The results were compared with some existing fin-body-interaction theories and an alteration to these theories is presented which improves their predictions for rather blunt bodies at high Mach numbers.

SYMBOLS

C_N	normal-force coefficient based on frontal area of the body, $\frac{N}{qS}$
ΔC_N	incremental normal-force coefficient due to the addition of fins to the body
C_m	pitching-moment coefficient about the base of the body based on frontal area and maximum diameter of the body, $\frac{M}{qSd}$
N	normal force
M	pitching moment about the base of the body
q	free-stream dynamic pressure
S	frontal area of the body
d	maximum diameter of the body
c.p.	center-of-pressure location in calibers from the base of the body
α	angle of attack, deg

APPARATUS

The tests were conducted in the Langley 9- by 9-inch Mach number 4 blowdown tunnel which is described in reference 2. The settling-chamber pressure, which was held constant by a pressure-regulating valve, and the corresponding air temperature were continuously recorded on film during each run. Wire strain-gage balances mounted on stings and located inside the models were used to measure normal force and pitching moment.

MODELS

The models consisted of fineness-ratio-9 and -12 ogive-cylinder bodies of revolution with and without two horizontal fins of three plan forms. The trailing edges of all the fins were normal to the body axis and were located even with the base of the body (see fig. 1). The ogival nose of both bodies was formed by one-half of an arc of radius 9.431 inches and chord of 6.06 inches. The afterbody was a 1-inch-diameter cylinder of length 5.97 inches for fineness ratio 9 and 8.97 inches for fineness ratio 12. The fin plan forms were rectangular, half-delta, and the trapezoidal plan form of the vertical stabilizer of the Bell X-2 airplane. All fins had an exposed area of 4.74 square inches and were $\frac{1}{10}$-inch-thick flat plates, with a $\frac{9}{16}$-inch symmetrical leading-edge wedge measured parallel to the body axis. The rectangular and half-delta fins had an aspect ratio of 1.072. The trapezoidal fin had an aspect ratio of 2.384 and had a root chord to body length ratio (for the fineness-ratio-9 body) equal to that of the Bell X-2 airplane. The leading edge of the half-delta fin was swept back 75°; whereas the leading edge of the trapezoidal fin was swept back approximately 40.5°.

TESTS

Tests were made to obtain the normal-force and pitching-moment coefficients of the bodies alone and of the finned configurations with the fins oriented in a plane perpendicular to the angle-of-attack plane. The tests were run at humidities below 1.0×10^{-5} pounds of water vapor per pound of dry air, which are believed to be low enough to eliminate any appreciable condensation effects. The fineness-ratio-9 and -12 configurations were tested at Reynolds numbers based on body length of 16.8×10^6 and 22.3×10^6, respectively. All configurations except

the fineness-ratio-12 finned bodies were tested through an angle-of-attack range of 0° to 10°. The latter configurations were tested only to 7° because of the strain-gage-balance measuring limits.

Schlieren photographs of the flow around the models were obtained by use of a system incorporating a spark-discharge light source of 1-microsecond duration. The actual angles of attack under running conditions were measured from the schlieren negatives by use of an optical comparator.

PRECISION OF DATA

The uncertainties involved in obtaining the aerodynamic coefficients and the center-of-pressure locations have been analyzed. It was determined that the existing average variation of stream Mach number, which is -0.01 per inch in the downstream direction, would cause the experimental center-of-pressure locations to be 0.05 caliber too far back on the body; however, this correction was not applied to the data because of its small size and approximate nature. The probable uncertainties in the data due to the above effect and the accuracy limitations of the balance and the settling-chamber-pressure recorder are listed in the following table:

	Probable uncertainty
C_N	±0.01
C_m	±0.05
Center of pressure	±0.1 caliber
α, deg	±0.1°

RESULTS AND DISCUSSION

Theoretical Methods

The total normal force and pitching moment of a finned-body configuration may be broken down into: the component of each due to the body alone; the components due to the fins alone; the components acting on the fins due to the presence of the body; and the components acting on the body due to the presence of the fins.

The theoretical methods of references 3, 4, and 5 may be used in their entirety to obtain the components listed above when the body and the Mach number are such that slender-body theory can be applied.

However, the test body at the test Mach number cannot be treated by slender-body theory, since the body apex half-angle is greater than the free-stream Mach angle; therefore, predictions of the normal-force and pitching-moment coefficients for the bodies without fins were obtained by the methods of references 6 and 7. The semiempirical method of reference 6 is based on potential theory, is not strictly applicable to bodies as blunt as the test bodies at Mach number 4, and is used here only for comparison with the correlation of experimental data presented in reference 7. This correlation was obtained from experimental data on conical and ogival-nosed bodies of fineness ratio 3.5 to 17 through the Mach number range from 2 to 4.31.

The fin and fin-body-interaction forces were estimated by the methods of references 3, 4, and 5, and were combined with the predictions of reference 7 for the body alone to give predictions of the normal-force and pitching-moment coefficients of the complete configurations. The predictions of the methods of Lagerstrom and Van Dyke (ref. 3) and Nielsen and Kaattari (ref. 5) for the fin-body-interaction forces of the configurations tested are so nearly identical that they plot as practically the same line. This result is coincidental, since Lagerstrom and Van Dyke do not take into account the force on the body caused by the fin. They use an upwash term, however, which is larger than that used by Nielsen and Kaattari so that their predictions of the forces on the fins due to the body are practically identical, (for these configurations) with the sum of Nielsen and Kaattari's predictions of the same factor and the force on the body due to the fins.

When the results of references 3 to 5 were used to predict the pitching moments of the configurations, it was assumed that the fin normal force and the normal force on the fins due to the body acted at the centroid of area of the fins. The normal force on the body due to the fins predicted by references 4 and 5 was assumed to act at the centroid of the area enclosed by the Mach line from the intersection of the fin leading edge and the body, the fin root, and the base of the body.

Experimental Results

Normal force.- Figure 2 presents the experimental and predicted variations of normal-force coefficient with angle of attack for all configurations. The method of reference 6 gives rather poor estimates of the normal-force coefficients throughout the angle-of-attack range for both the fineness-ratio-9 and -12 bodies (fig. 2), as might be expected because of the limitations of the method. Use of the correlation of reference 7 gives excellent predictions of body-normal-force coefficients up to about an angle of attack of 6° but somewhat underestimates

the coefficients at higher angles and increasingly underestimates them with increasing fineness ratio.

The three methods of predicting the normal-force coefficients (refs. 3 to 5, each in combination with ref. 7) gave about the same agreement with experiment for the rectangular and the trapezoidal models, very good agreement at low angles of attack, and about 10 percent low at the higher angles of attack. For the delta-finned configurations, combining references 3 and 5 with reference 7 gave very good agreement throughout the test angle-of-attack range; however, in this case, the predicted normal-force coefficients were slightly greater than experiment. The method of reference 4 combined with reference 7 gave predictions of the normal-force coefficients that were still higher than the predictions of the other methods. It might be expected that the experimental values for the delta-finned configurations would be somewhat lower than the theoretical predictions since, although this fin plan form has a slightly supersonic leading edge and was so considered in the theoretical calculations, it is actually operating with a detached shock because of its thickness, as is shown by the schlieren photographs of figure 3, so that the normal force becomes less than the two-dimensional value. A comparison of the experimental results for the finned-body configurations (fig. 4) showed that the trapezoidal-finned configurations had slightly higher normal-force-curve slopes than the rectangular- and the delta-finned configurations. This variation of normal-force-curve slope might be expected since the trapezoidal fin has a higher theoretical normal-force-curve slope than the rectangular fin because it has a larger percentage of two-dimensional-flow area and since the normal-force-curve slope of the delta fin might be expected to be lower than the two-dimensional value because of the region of subsonic flow behind the detached shock at the leading edge.

The effect of increasing the fineness ratio from 9 to 12 was to increase the normal-force coefficients at most angles of attack on each of the configurations by an amount approximately equal to that predicted for the body alone by the method of reference 7. The ΔC_N contributed by the fins was about the same for both fineness ratios (fig. 5); therefore the increments in normal force due to the body upwash and fin-body-interference effects are about the same for both fineness-ratio models. The ΔC_N is 25 to 50 percent greater than the theoretical two-dimensional-fin normal-force coefficient, which is also plotted on figure 5.

For these data to be applicable to configurations having one vertical tail fin, the pressure fields on the body caused by the fins should not overlap. At small angles of attack, this condition can be investigated by assuming that the disturbances spread out on the surface of the body within free-stream Mach helices drawn from the leading edge

of the root chord of the fins. On this basis, the trapezoidal- and the rectangular-finned configurations are free of interference, but the half-delta-finned configurations are not. The possibility that the influence of the fins might be felt outside of the Mach helices through the boundary layer and the effect of the subsonic flow near the leading edge of the half-delta fins has not been investigated.

Pitching moment.- The theoretical curves of pitching-moment coefficient against normal-force coefficient for the body alone are compared with experimental values in figure 6, and it is evident that the method of reference 7 gives the better prediction of the stability of the bodies. The experimental moment curves for the finned configurations (fig. 6) of both fineness ratios show good agreement with the curves obtained by combining the predictions of reference 7 with those of references 3 to 5. Comparison of the experimental curves shows that the trapezoidal- or X-2-plan-form-finned configurations were the most stable of the three configurations tested and were followed in order of decreasing stability by the rectangular and the delta-finned configurations.

Center-of-pressure.- The experimental and predicted center-of-pressure positions for all configurations as determined from figure 6 are compared on figure 7. The experimental centers of pressure at $\alpha = 0^\circ$ were obtained from the slopes of large-scale plots of pitching-moment coefficient against normal-force coefficient and are indicated by the short horizontal lines on the $\alpha = 0^\circ$ axes of figure 7. Center-of-pressure locations obtained from the actual test points are also included. The method of reference 7 gives good agreement with experiment for the bare-body configurations; whereas that of reference 6 gives predictions which are from 1/2 to 1 caliber too far forward.

Predictions of center-of-pressure location for the finned bodies of both fineness ratios obtained by combining the methods of reference 7 with those of references 3 to 5 agree with the experimental results at $\alpha = 0^\circ$ within 0.25 caliber (fig. 7), except for the predictions of reference 7 combined with those of reference 4 for the delta-finned configurations. The centers of pressure of the rectangular- and delta-finned configurations are, respectively, about 1/4 and 1/2 caliber forward of the centers of pressure of the trapezoidal-finned configurations (fig. 8). This variation of center-of-pressure location corresponds to the variation of the fin centroid of area. From figure 8 it can be seen that the centers of pressure of the normal-force increments due to the fins are slightly forward of the centroids of area of the fins.

From the results of these tests, some observations concerning the design of tail fins to give maximum stability to body-tail configurations at Mach number 4 can be made. The centroid of area of the fin should

be as far rearward as possible and, in order to assure a maximum normal-force-curve slope, the fin should have no subsonic edges and the leading-edge sweep and leading-edge profile should be so combined that the leading-edge shock is not detached. This describes a highly tapered swept fin with a leading-edge angle small enough to permit shock attachment. Considerations of air-frame design and changes in directional stability with Mach number indicate that aspect ratios as low as possible, consistent with the other requirements, are desirable.

CONCLUSIONS

An investigation has been made into the effects of fin plan form on the static stability of fineness-ratio-9 and -12 fin-body combinations at Mach number 4.06 and Reynolds numbers of 16.8×10^6 and 22.3×10^6 based on body lengths. Analysis of the results of this investigation indicated that:

1. The normal-force and pitching-moment coefficients of the test configurations could be predicted rather accurately by combining the results of a correlation of experimental data for the body alone with theoretical fin and fin-body-interaction forces.

2. The trapezoidal- or Bell X-2-finned configurations showed the most stability and were followed in order of decreasing stability by the rectangular configurations and the delta-finned configurations. The X-2 configurations had both the highest normal-force-curve slopes and the most rearward centers of pressure.

3. The centers of pressure of the finned configurations varied as the location of the centroids of fin-plan-form area.

Langley Aeronautical Laboratory
National Advisory Committee for Aeronautics
Langley Field, Va.

REFERENCES

1. Spearman, M. Leroy, and Robinson, Ross B.: The Aerodynamic Characteristics of a Supersonic Aircraft Configuration With a 40° Sweptback Wing Through a Mach Number Range From 0 to 2.4 As Obtained From Various Sources. NACA RM L52A21, 1952.

2. Ulmann, Edward F., and Lord, Douglas R.: An Investigation of Flow Characteristics at Mach Number 4.04 Over 6- and 9-Percent-Thick Symmetrical Circular-Arc Airfoils Having 30-Percent-Chord Trailing-Edge Flaps. NACA RM L51D30, 1951.

3. Lagerstrom, P. A., and Van Dyke, M. D.: General Considerations About Planar and Non-Planar Lifting Systems. Rep. No. SM-13432, Douglas Aircraft Co., Inc., June 1949.

4. Morikawa, George: Supersonic Wing-Body Lift. Jour. Aero. Sci., vol. 18, no. 4, Apr. 1951, pp. 217-228.

5. Nielsen, Jack N., and Kaattari, George E.: Method for Estimating Lift Interference of Wing-Body Combinations at Supersonic Speeds. NACA RM A51J04, 1951.

6. Allen, H. Julian: Estimation of the Forces and Moments Acting on Inclined Bodies of Revolution of High Fineness Ratio. NACA RM A9I26, 1949.

7. Grimminger, G., Williams, E. P., and Young, G. B. W.: Lift on Inclined Bodies of Revolution in Hypersonic Flow. Jour. Aero. Sci., vol. 17, no. 11, Nov. 1950, pp. 675-690.

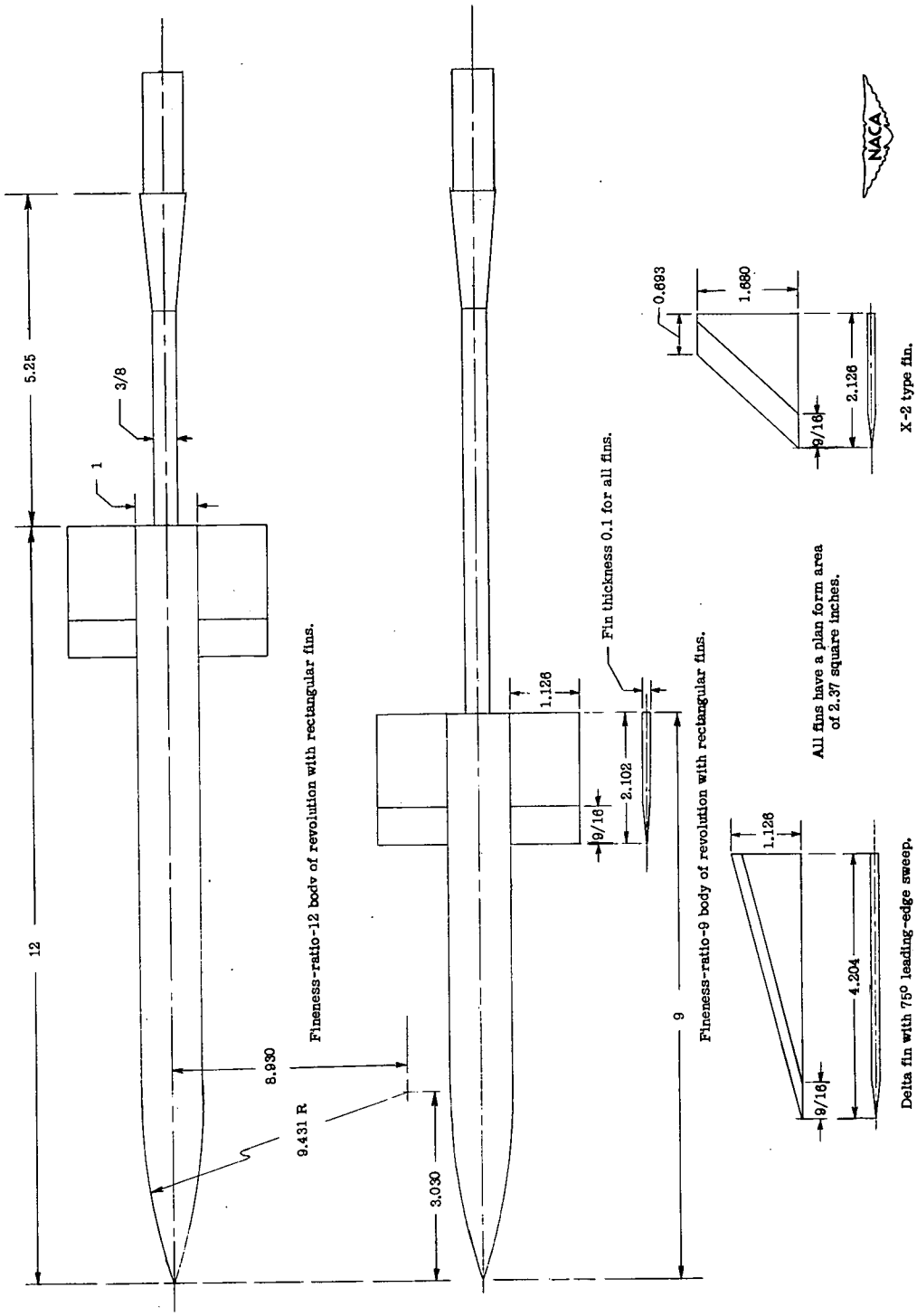

Figure 1.- Dimensions of the models and the sting support. All dimensions are in inches.

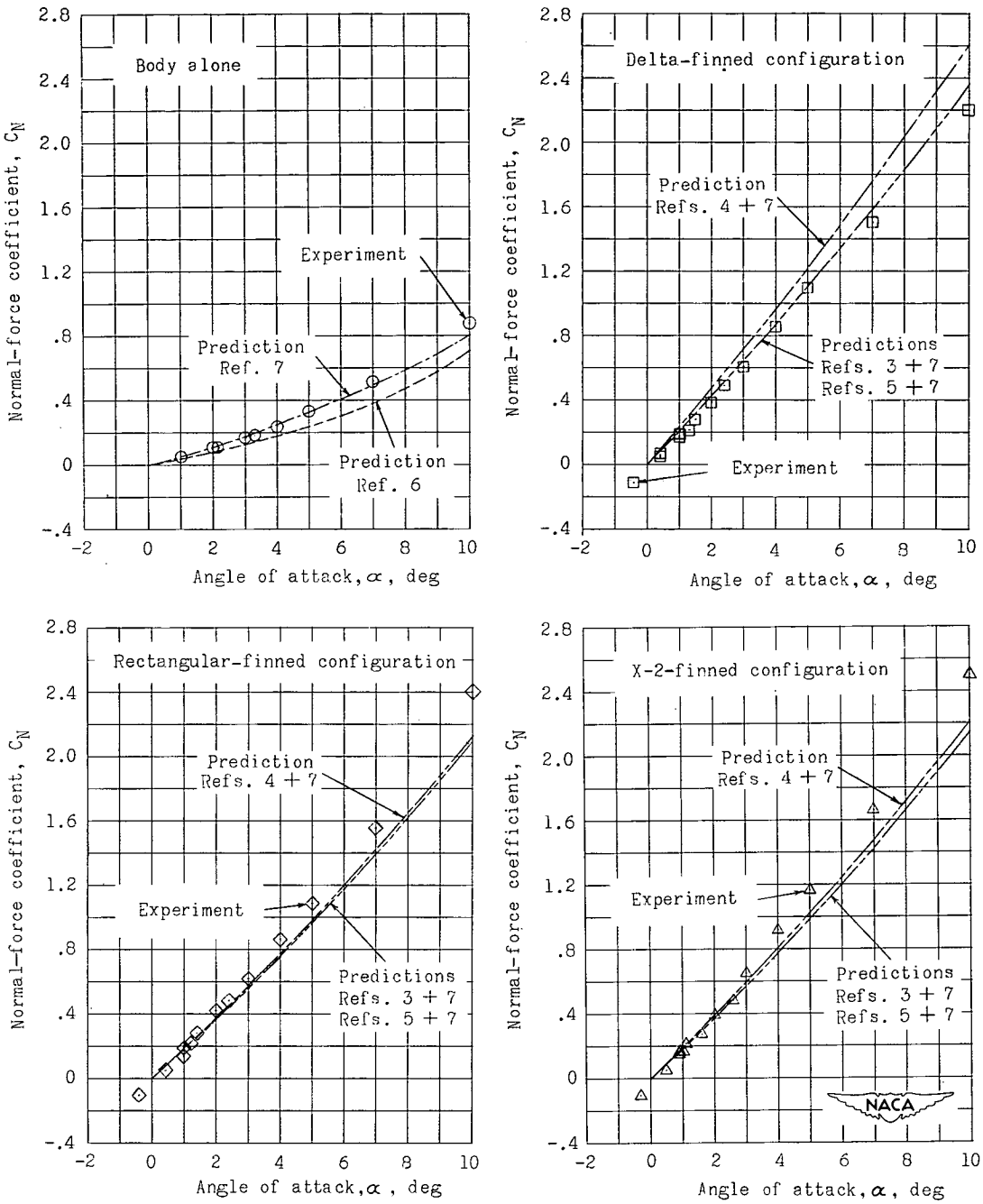

(a) Fineness ratio 9.

Figure 2.- Normal-force coefficients for body alone and finned body configurations at M = 4.06 and at a Reynolds number of 16.8×10^6 for the fineness-ratio-9 configurations and 22.3×10^6 for the fineness-ratio-12 configurations.

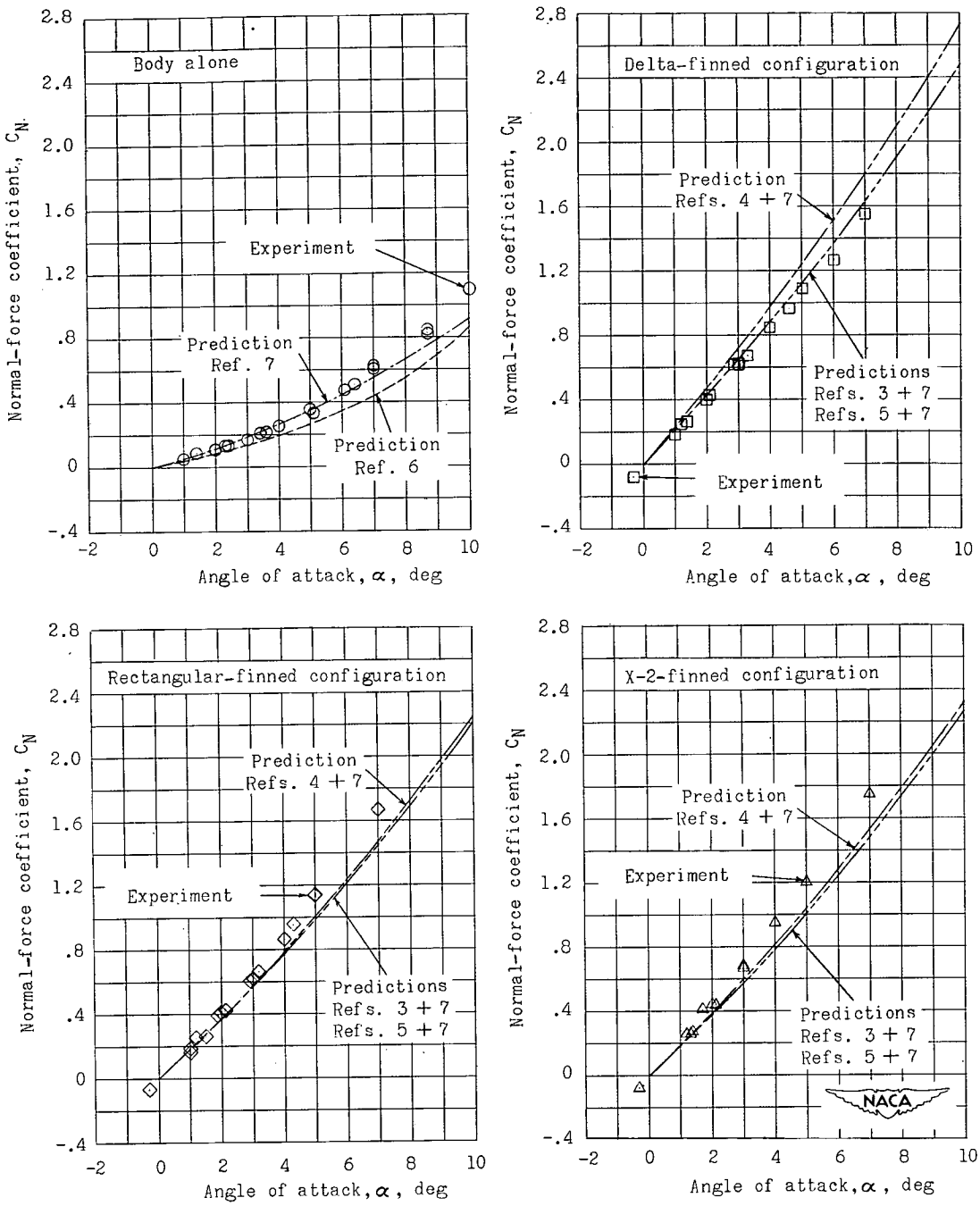

(b) Fineness ratio 12.

Figure 2.- Concluded.

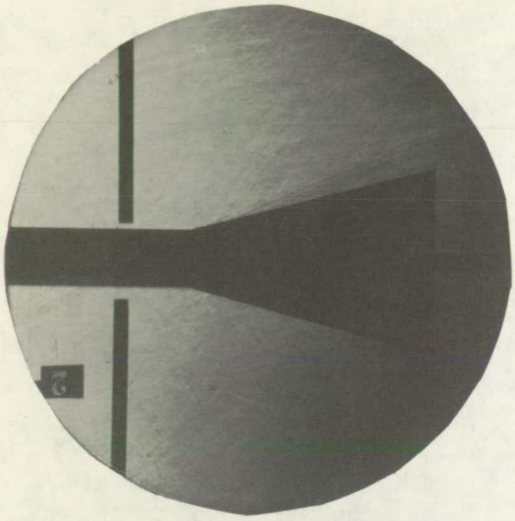

No flow

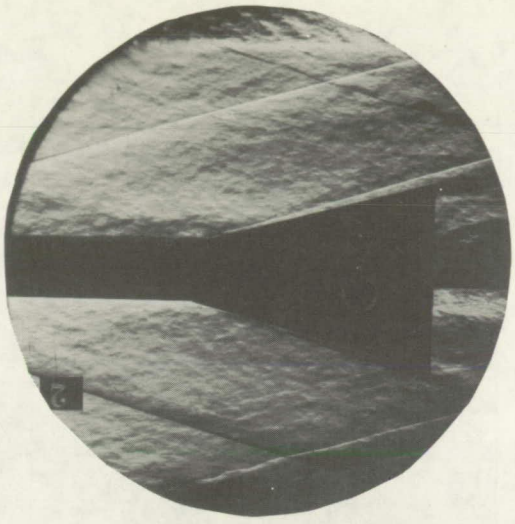

Delta-finned configuration

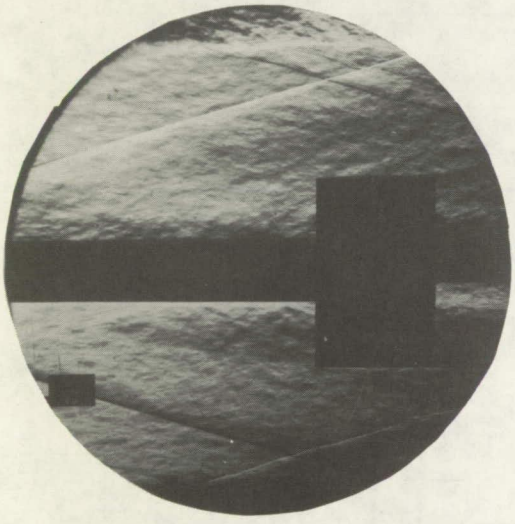

Rectangular-finned configuration

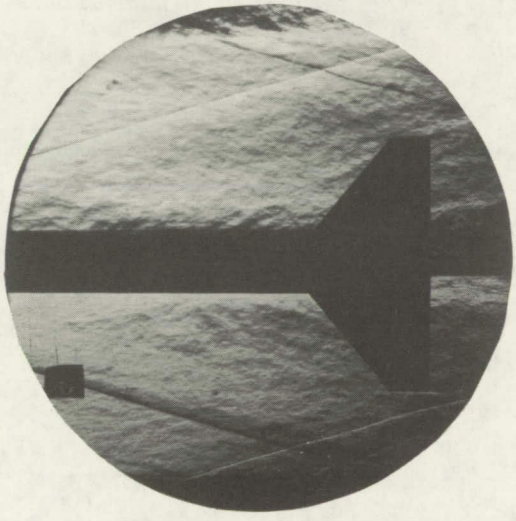

X-2-finned configuration

NACA

L-75089

Figure 3.- Plan-form schlieren photographs of the three finned configurations at zero angle of attack and zero angle of yaw at $M = 4.06$ and at a Reynolds number of 22.3×10^6.

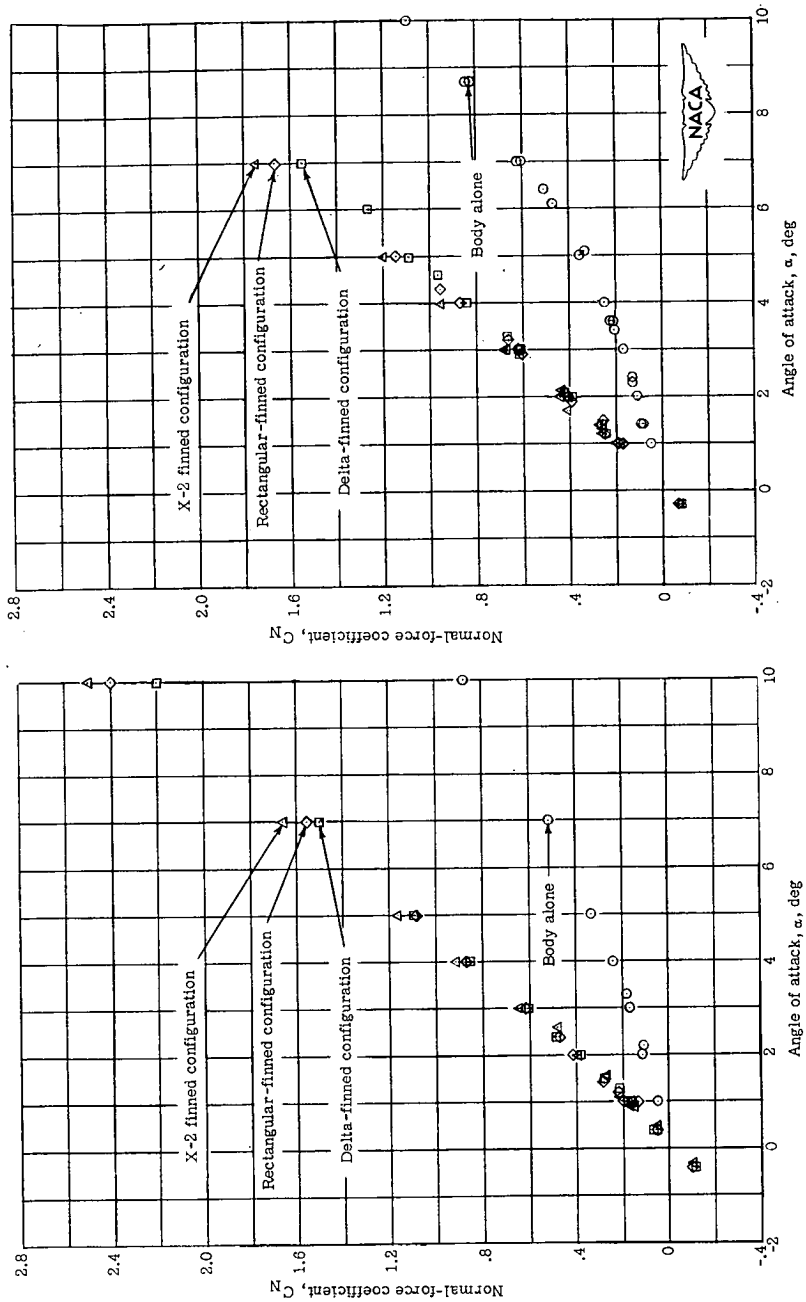

(a) Fineness ratio 9.

(b) Fineness ratio 12.

Figure 4.- Comparison of experimental normal-force coefficients for the fineness-ratio-9 and fineness-ratio-12 body alone and finned-body configurations at $M = 4.06$ and at a Reynolds number of 16.8×10^6 for the fineness-ratio-9 configurations and 22.3×10^6 for the fineness-ratio-12 configurations.

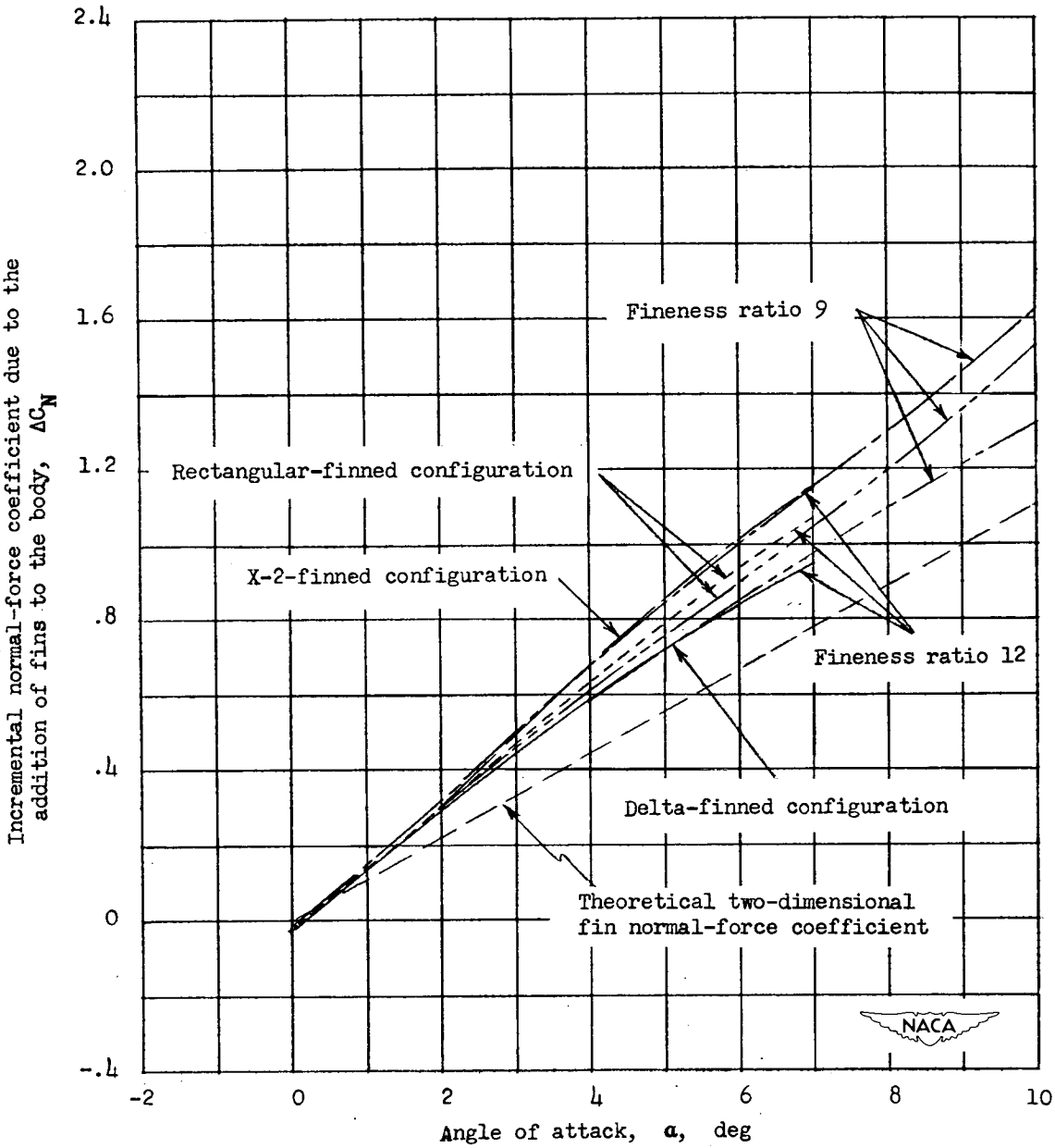

Figure 5.- Comparison of increments in normal force contributed by the tail fins for all configurations at $M = 4.06$ and at a Reynolds number of 16.8×10^6 for the fineness-ratio-9 configurations and 22.3×10^6 for the fineness-ratio-12 configurations.

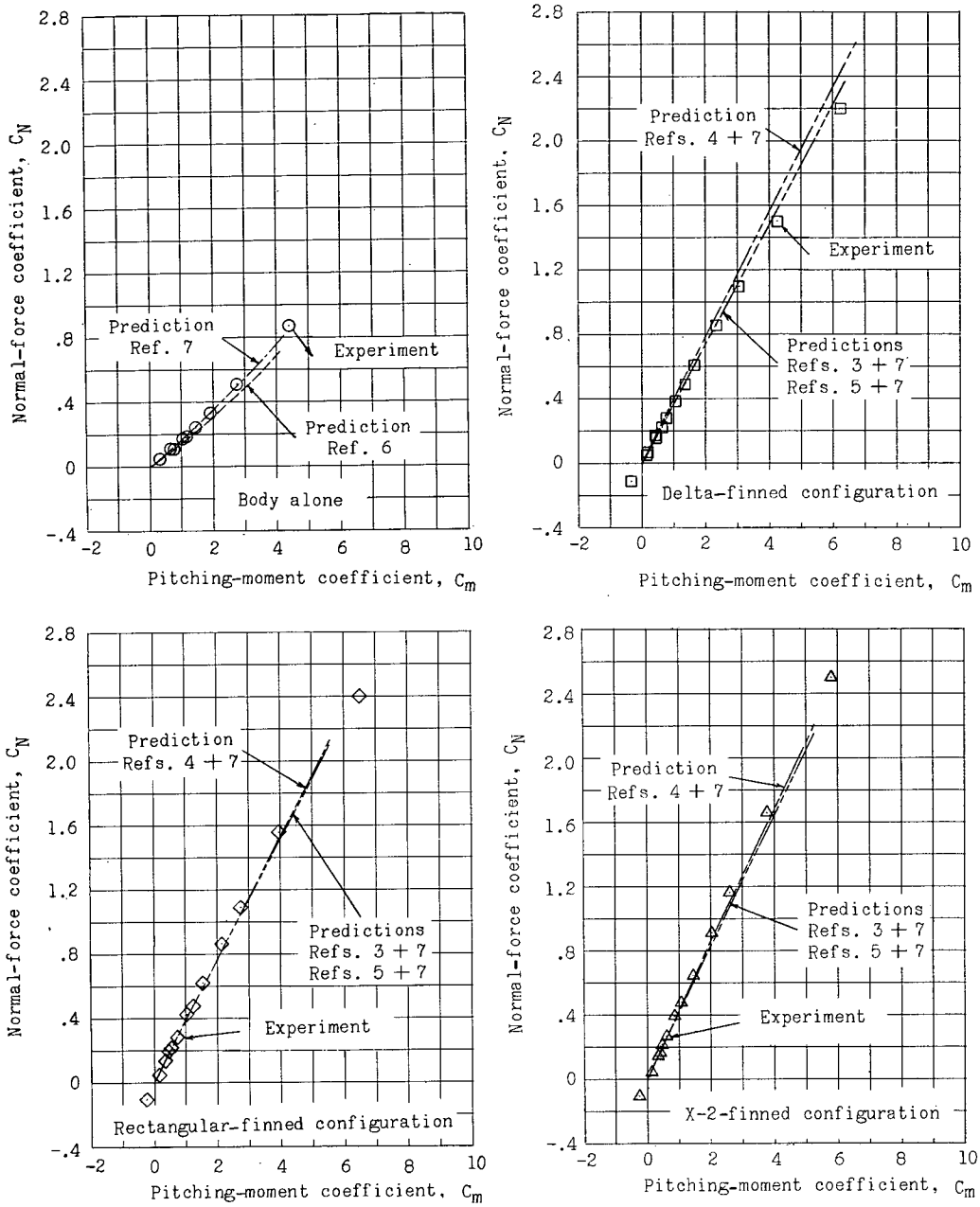

(a) Fineness ratio 9.

Figure 6.- Pitching-moment coefficients for body alone and finned-body configurations at $M = 4.06$ and at a Reynolds number of 16.8×10^6 for the fineness-ratio-9 configurations and 22.3×10^6 for the fineness-ratio-12 configurations.

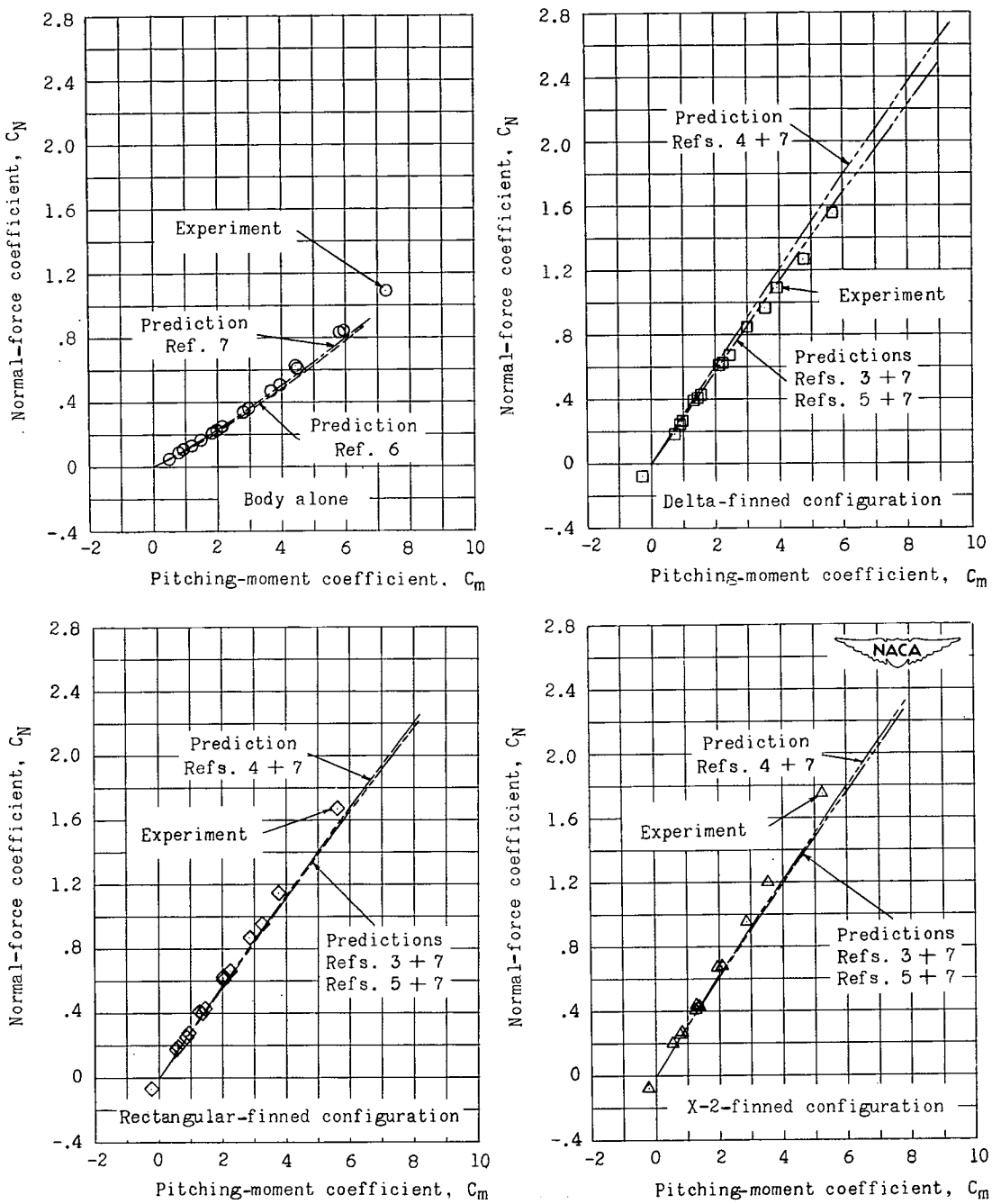

(b) Fineness ratio 12.

Figure 6.- Concluded.

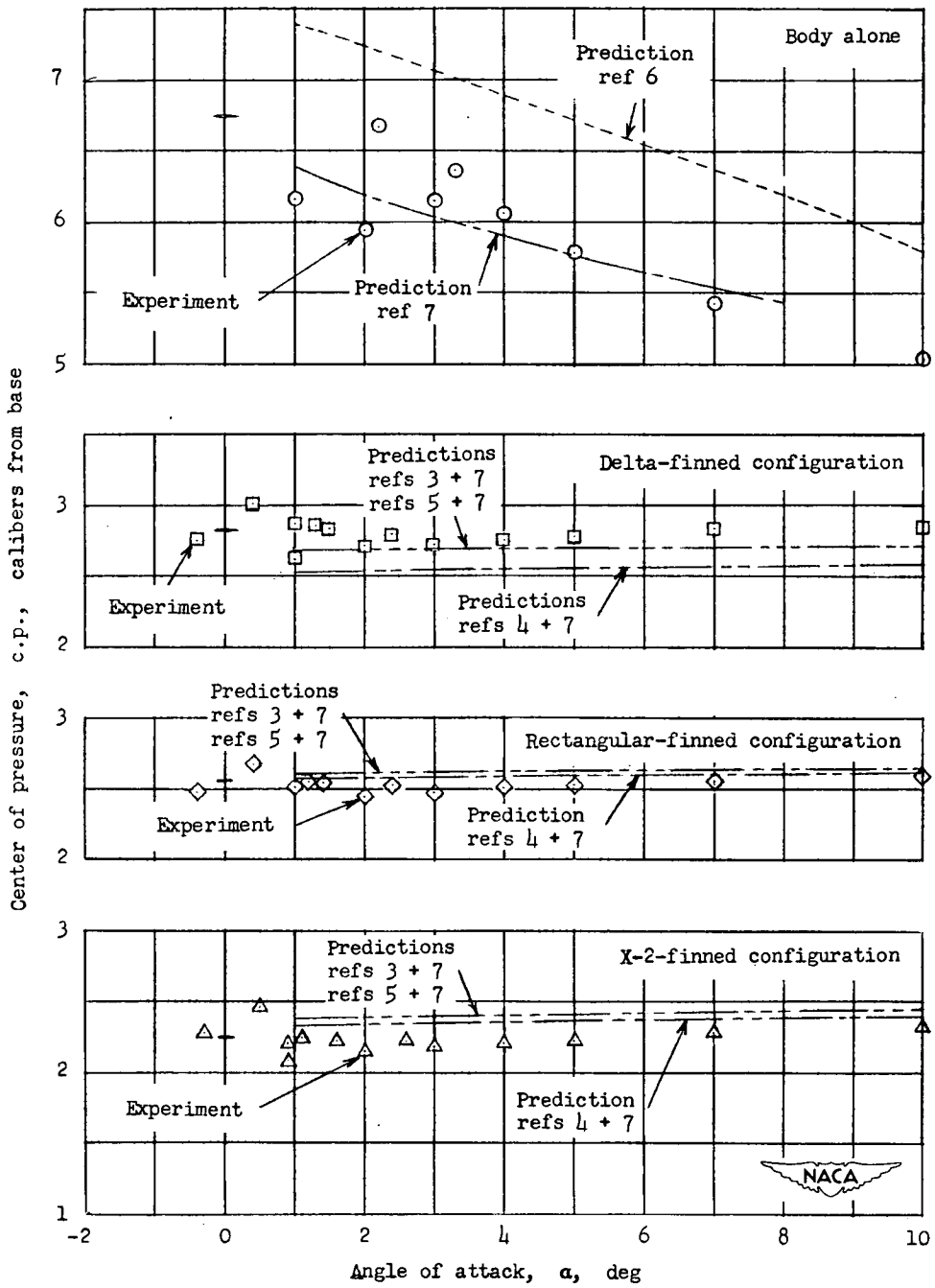

(a) Fineness ratio 9.

Figure 7.- Center-of-pressure position for body alone and finned-body configurations at $M = 4.06$ and at a Reynolds number of 16.8×10^6 for the fineness-ratio-9 configurations and 22.3×10^6 for the fineness-ratio-12 configurations.

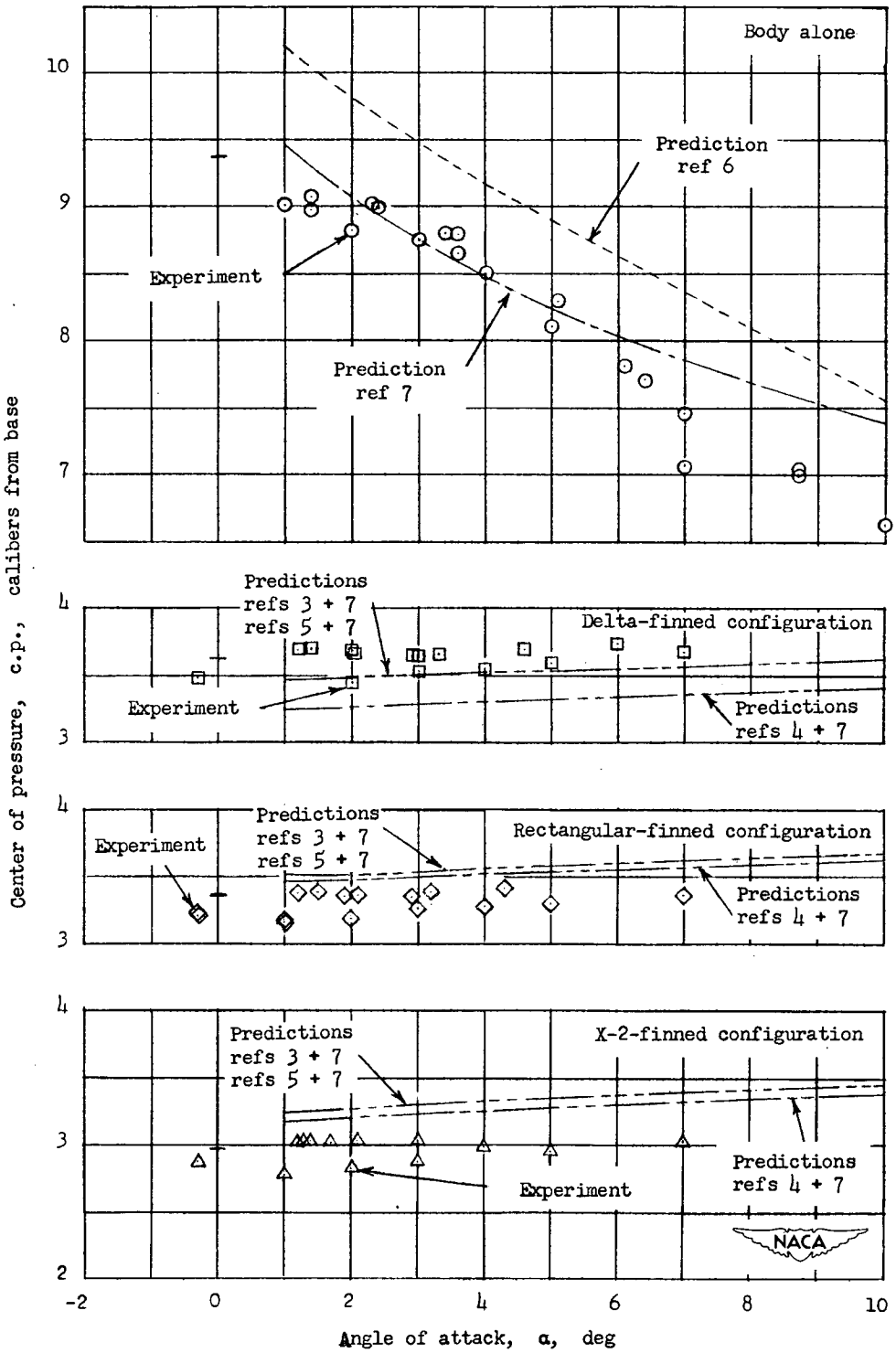

(b) Fineness ratio 12.

Figure 7.- Concluded.

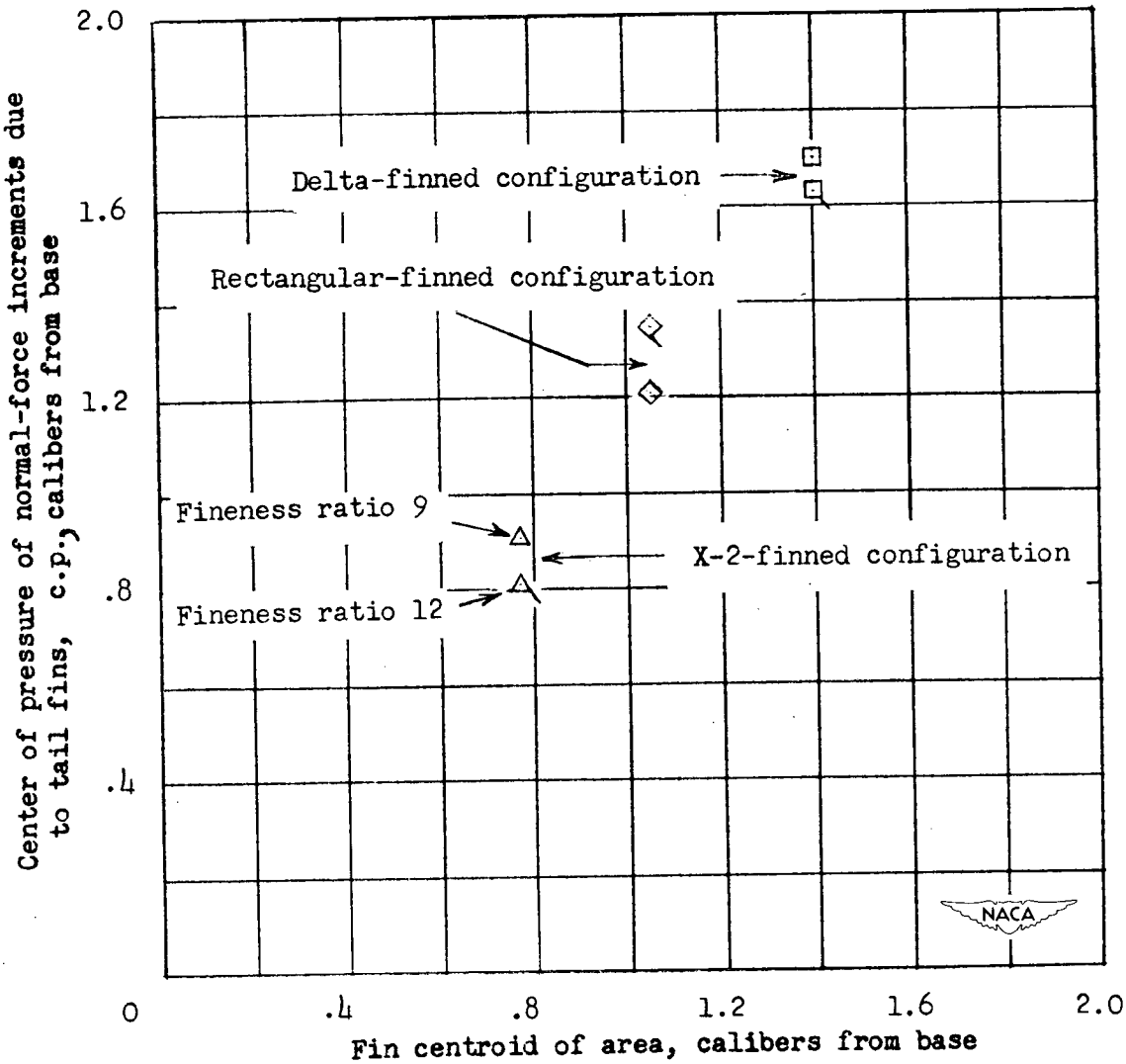

Figure 8.- Comparison of centers of pressure of normal-force increments due to tail fins with centroids of area of tail fins at $M = 4.06$ and at a Reynolds number of 16.8×10^6 for the fineness-ratio-9 configurations and 22.3×10^6 for the fineness-ratio-12 configurations.